Limiting Light Dark Matter with Luminous Hadronic Loops

Melissa Diamond[*], Christopher V. Cappiello[†], Aaron C. Vincent[‡] and Joseph Bramante[§]

Department of Physics, Engineering Physics, and Astronomy, Queen's University, Kingston, Ontario, K7N 3N6, Canada;
The Arthur B. McDonald Canadian Astroparticle Physics Research Institute, Kingston, Ontario, K7L 3N6, Canada
and Perimeter Institute for Theoretical Physics, Waterloo, Ontario, N2L 2Y5, Canada

Dark matter is typically assumed not to couple to the photon at tree level. While annihilation to photons through quark loops is often considered in indirect detection searches, such loop-level effects are usually neglected in direct detection, as they are typically subdominant to tree-level dark-matter–nucleus scattering. However, when dark matter is lighter than around 100 MeV, it carries so little momentum that it is difficult to detect with nuclear recoils at all. We show that loops of low-energy hadronic states can generate an effective dark-matter–photon coupling, and thus lead to scattering with electrons even in the absence of tree-level dark-matter–electron scattering. For light mediators, this leads to an effective fractional electric charge that may be very strongly constrained by astrophysical observations. Current and upcoming searches for dark-matter–electron scattering can thus set limits on dark-matter–proton interactions down to 1 MeV and below.

Introduction.—Although dark matter (DM) comprises most of the mass in the Universe, how (and whether) it interacts nongravitationally is completely unknown [1–3]. Direct detection bounds on DM, as well as astrophysical and cosmological constraints, are often presented in a "model-independent" way, e.g., as limits on dark matter's nonrelativistic scattering cross section with protons or electrons, rather than limits on a larger set of model parameters. In such a framework, limits on dark matter's interactions with different standard model (SM) particles are often treated independently. There are, of course, exceptions—DM-proton and DM-neutron cross sections are often assumed to be identical to avoid isospin violation— but, for example, limits on DM-electron scattering are often set assuming that DM-nucleon scattering is negligible, and vice versa.

However, even DM, which only interacts with one SM particle at tree level, can interact with others at loop level. As a classic example, Ref. [4] showed how fermionic loops could generate an effective electromagnetic charge. This is commonly cited in literature on dark photons and milli-charged DM [5–18], and explicit calculations of quark-, lepton-, or W-loop-induced processes may be found in many references on indirect detection, collider searches, and, to a lesser extent, direct detection ([19–38], see also [39,40]). In works focused on indirect detection or collider searches, the energies are typically high enough that QCD is perturbative, and loops of quarks can be computed directly.

In this Letter, we explicitly compute the DM-photon interaction induced by DM couplings to hadronic states at low energy, where the relevant degrees of freedom are not quarks, but mesons and baryons. This is in contrast with much of the literature on kinetically mixed dark photons, which treats the mixing between the photon and dark photon as a phenomenological parameter that is generated at much higher energy scales. We show that such loop-level couplings can produce detectable event rates in direct detection experiments, and/or induce a non-negligible effective charge for the DM, in a wide range of sub-GeV parameter space. We thus set new limits on sub-GeV dark matter's coupling to protons.

This Letter is organized as follows. In the next section, "Effective DM-electron interactions," we review the ideas of Ref. [4], and discuss the types of interaction that yield nonzero results. We then introduce our model and the effective Lagrangians used to describe dark matter's inter-actions with hadronic states, and compute the induced interactions with photons and electrons. In the "Results" section, we compute new constraints on sub-GeV DM. In the concluding section, we discuss the implications of our results. Detailed descriptions of the calculations performed in this work can be found in the Supplemental Material [41].

Effective DM-electron interactions.—Suppose that DM is a fermion, χ, that interacts with protons via a new vector mediator that we refer to as Z' [the tree-level diagram is
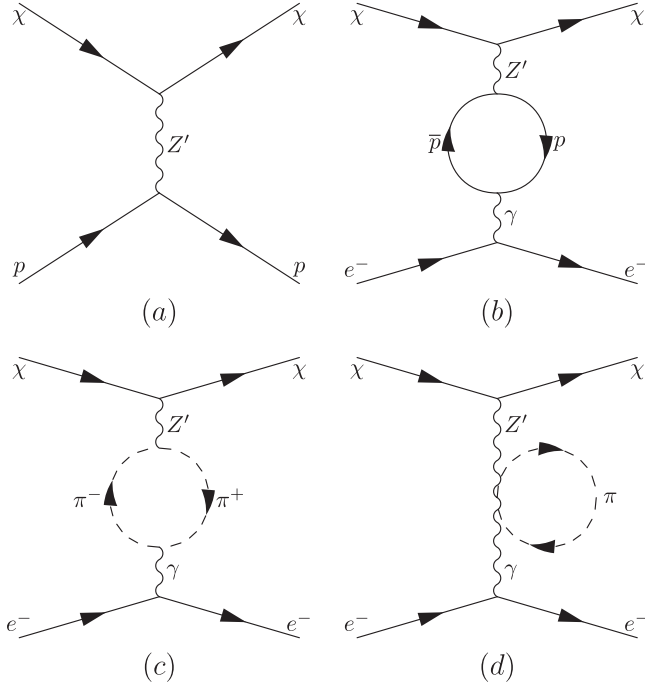
FIG. 1. Feynman diagrams utilized in this work. The tree-level diagram (a) captures DM-proton scattering. The loop-level diagrams (b)–(d) show DM-electron scattering that results from the DM-proton interaction.

shown in Fig. 1(a)]. A proton loop then induces a mixing between the Z' and the photon, as well as a DM-electron interaction, as shown in Fig. 1(b). If Z' is massless, the result is an effective charge for the DM, as derived by Ref. [4]. A massive Z' will still mix with the photon, but the different momentum dependence means that the DM no longer behaves as a truly millicharged particle.

If the Z' couples to protons, then on a more fundamental level it must couple to the constituent quarks (or gluons), and thus also to mesons. In fact, the more typical approach to such hadronic corrections would be to use loops of pions [Figs. 1(c) and 1(d)], whose masses are below the QCD scale and for which the framework of chiral effective field theory (ChEFT) can readily be applied. The use of pion loops in this context is similar to their role in hadronic vacuum polarization, notably in the context of muon $g - 2$ (see Ref. [42] for a detailed review).

In this work, we include both proton and light pseudo-scalar meson (specifically pion and kaon) loops in order to compute the induced mixing between the Z' and photon. We take inspiration from Ref. [43], which showed that nucleons could be included in the framework of chiral perturbation theory while preserving chiral power counting.

We consider only the case of a vector mediator, because the diagrams shown in Figs. 1(b)–1(d) vanish for a scalar or axial vector mediator (see Ref. [24]). An analogous interaction between DM and electrons in the scalar case can be induced at the 2-loop level [24], or by instead

mixing with the Higgs at 1 loop; however, both are suppressed compared to the 1-loop vector mixing with the photon.

Below, we estimate the effective DM-electron scattering cross section that results from hadronic loops. We focus on DM in the mass range accessible to electron recoil searches, but difficult to probe using nuclear recoil searches ($1 \text{ MeV} \lesssim m_\chi \lesssim 100 \text{ MeV}$) [44–51]. At eV-scale energies, the typical kinetic energy of MeV-scale mass dark matter, quarks are confined into baryons and light mesons, and their behavior is best described using ChEFT. Using a shared underlying description of the DM-quark interaction we estimate both the DM-proton and DM-meson coupling. These allow us to estimate tree-level DM-proton cross section and the corresponding 1-loop DM-electron cross section.

Interactions between a dark fermion and quarks through a vector mediator can be described by

$$\mathcal{L} \supset \sum_q \alpha_q Z'_\mu q \gamma^\mu \bar{q} + g_\chi Z'_\mu \chi \gamma^\mu \bar{\chi}, \qquad (1)$$

where q, α_q, and g_χ represent the quarks, the coupling of each quark specie to Z'_μ, and the coupling between Z' and the DM, respectively.

At low momentum, the resulting effective proton interaction can be determined following Sec. B.2 of Ref. [52]:

$$\mathcal{L} \supset (2\alpha_u + \alpha_d) Z'_\mu p \gamma^\mu \bar{p}. \qquad (2)$$

The meson interaction terms can be derived from the ChEFT Lagrangian. The relevant lowest order interaction term in the ChEFT Lagrangian is [53]

$$L \supset \frac{F^2}{4} \text{Tr}(D_\mu U D^\mu U^\dagger), \qquad (3)$$

where $U = e^{(i/F)\pi}$ contains the light meson octet

$$\pi = \begin{pmatrix} \pi^0 + \frac{\eta_8}{\sqrt{3}} & \sqrt{2}\pi^+ & \sqrt{2}K^+ \\ \sqrt{2}\pi^- & -\pi^0 + \frac{\eta_8}{\sqrt{3}} & \sqrt{2}K^0 \\ \sqrt{2}K^- & \sqrt{2}\bar{K}^0 & -\frac{2}{\sqrt{3}}\eta_8 \end{pmatrix}. \qquad (4)$$

F is the pion decay constant. Interactions with external vector fields (namely the photon or Z') are captured in the derivative terms

$$D_\mu U = \partial_\mu U - iv_\mu U + iUv_\mu,$$
$$D_\mu U^\dagger = \partial_\mu U^\dagger + iU^\dagger v_\mu - iv_\mu U^\dagger, \qquad (5)$$

where the matrix v_μ captures the interactions between external vectors and the quarks that compose the light mesons. Setting $v_\mu = Z'_\mu \text{diag}(\alpha_u, \alpha_d, \alpha_s)$ accounts for the

Z' coupling to quarks shown in Eq. (1). While taking $v_\mu = eA_\mu \text{diag}(\frac{2}{3}, -\frac{1}{3}, -\frac{1}{3})$ captures electromagnetic interactions.

Expanding the chiral Lagrangian (3) gives the following interaction terms between light mesons, photons, and Z':

$$\mathcal{L} \supset i(\alpha_u - \alpha_d)Z'_\mu(\pi^- \partial^\mu \pi^+ - \pi^+ \partial^\mu \pi^-)$$
$$+ i(\alpha_u - \alpha_s)Z'_\mu(K^- \partial^\mu K^+ - K^+ \partial^\mu K^-)$$
$$+ ieA_\mu(\pi^- \partial^\mu \pi^+ - \pi^+ \partial^\mu \pi^-)$$
$$+ ieA_\mu(K^- \partial^\mu K^+ - K^+ \partial^\mu K^-) + 2e(\alpha_u - \alpha_d)Z'_\mu A^\mu \pi^+ \pi^-$$
$$+ 2e(\alpha_u - \alpha_s)Z'_\mu A^\mu K^+ K^-. \quad (6)$$

Using these interaction terms we calculate the χp scattering cross section at tree level and the χe scattering cross section at loop level resulting from the diagrams shown in Fig. 1. These calculations are shown in more detail in the Supplemental Material.

At tree-level and low-momentum exchange

$$\frac{d\sigma_{\chi p}}{d\Omega} = \frac{g_\chi^2 (2\alpha_u + \alpha_d)^2 \mu_{\chi p}^2}{4\pi^2 (m_{Z'}^2 - t)^2}, \quad (7)$$

where $\mu_{ab} = m_a m_b / (m_a + m_b)$ represents the reduced mass of two particles with masses m_a and m_b and $m_{Z'}$ is the Z' mass.

The χe cross section at 1 loop is

$$\frac{d\sigma_{\chi e}}{d\Omega} = \frac{d\sigma_{\chi p}}{d\Omega} \frac{e^2}{2304\pi^4 (2\alpha_u + \alpha_d)^2} \left(\frac{\mu_{\chi e}}{\mu_{\chi p}}\right)^2 c_{\text{loop}}^2, \quad (8)$$

where

$$c_{\text{loop}} = 4(2\alpha_u + \alpha_d) \ln\left(\frac{4\pi e^{-\gamma_E} \mu^2}{m_p^2}\right)$$
$$+ (\alpha_u - \alpha_d) \ln\left(\frac{4\pi e^{-\gamma_E} \mu^2}{m_\pi^2}\right)$$
$$+ (\alpha_u - \alpha_s) \ln\left(\frac{4\pi e^{-\gamma_E} \mu^2}{m_K^2}\right). \quad (9)$$

The first term in c_{loop} comes from the proton loop as shown in Fig. 1(b); the second and third terms come from pion and kaon loops, respectively. The meson loop terms get contributions from diagrams of the form depicted in Figs. 1(c) and (d). Loop divergences are contained in the log terms, which depend on the mass of the particles in the loops (m_p, m_π, and m_K for protons, pions, and kaons, respectively) and a cutoff term logarithmic in μ. Following Ref. [43], we set $\mu = m_p$.

We perform our calculations in two mass limits: the heavy mediator limit, where the mediator mass is much larger than the typical momentum transfer, and the light mediator limit, where the mediator is much lighter than the

momentum transfer. For the dark matter masses we consider, the typical momentum transfer is O (keV). In the case of a heavy mediator, we integrate over scattering angles to find a relative total cross section of

$$\sigma_{\chi e} = \sigma_{\chi p} \frac{e^2}{2304\pi^4 (2\alpha_u + \alpha_d)^2} \left(\frac{\mu_{\chi e}}{\mu_{\chi p}}\right)^2 c_{\text{loop}}^2. \quad (10)$$

The factor $(e^2/2304\pi^4) \approx 4 \times 10^{-7}$. While this suppression seems substantial, the effective cross sections are large enough that current and upcoming electron recoil detectors will be able to observe or rule out DM inaccessible to current traditional nuclear recoil detectors.

For a massless mediator, the integrals of $d\sigma_{\chi e}/d\Omega$ and $d\sigma_{\chi p}/d\Omega$ over the scattering angle diverge. Although the inclusion of a mediator mass regulates this divergence, direct detection experiments are insensitive to this mass as long as it is small compared to the typical momentum transfer. Therefore, we instead report the ratio between $\bar{\sigma}_{\chi p}$ and $\bar{\sigma}_{\chi e}$, where

$$\bar{\sigma} \equiv 2 \frac{d\sigma}{d\cos\theta} \left(\frac{q}{q_{\text{ref}}}\right)^4. \quad (11)$$

Here, q represents the momentum exchanged between scattered particles, and q_{ref} is a reference momentum, usually taken to be $\sim \alpha m_e$ [13]. $\bar{\sigma}$ is Lorentz-invariant and typically used when discussing constraints on light mediator scattering. The resulting relation between light mediator cross sections is

$$\bar{\sigma}_{\chi e} = \bar{\sigma}_{\chi p} \frac{e^2}{2304\pi^4 (2\alpha_u + \alpha_d)^2} \left(\frac{\mu_{\chi e}}{\mu_{\chi p}}\right)^2 c_{\text{loop}}^2. \quad (12)$$

Hence, the ratio between the proton and electron cross sections does not depend on mass of the vector mediator. As the terms shared between proton and electron scattering diagrams divide out, the ratio between their cross sections also does not depend on the spin of the DM, or the Lorentz structure of its interaction with the vector mediator.

Results.—In direct detection literature, the interactions between DM and quarks that generate the DM-nucleon cross section are typically unspecified. Because we also include meson loops, recasting these limits requires a concrete choice for the couplings to individual quarks. In this section, we report our results for the case $\alpha_u = -\alpha_d$ and $\alpha_s = 0$, i.e., where the Z' couples to isospin. Results for an alternative case, $\alpha_u = \alpha_d = \alpha_s$, are shown in the Supplemental Material. The limits between these two cases differ by a factor of ~ 8. A different choice of couplings should not weaken the limits much beyond this range without fine tuning.

We use the SENSEI electron-recoil searches [47] to constrain the DM-proton cross section. SENSEI has reported some of the strongest limits on DM-electron
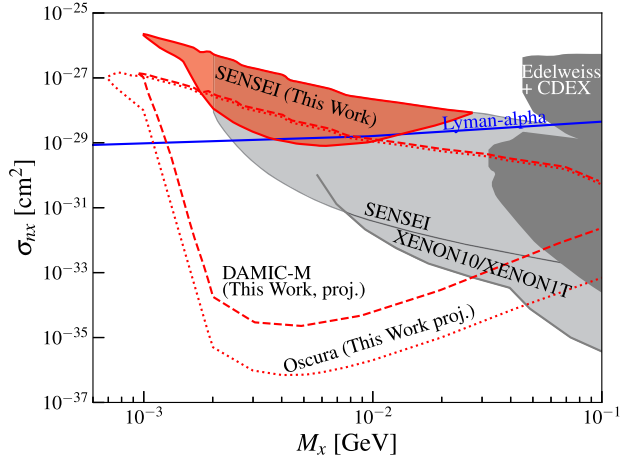
FIG. 2. Limits on the DM-nucleon cross section due to their loop-induced coupling to electrons. Interactions via a heavy vector mediator with $\alpha_u = -\alpha_d$ and $\alpha_s = 0$. Our recast constraint from SENSEI [47] is shown in red. The regions outlined in red dashed and dotted lines will be accessible to DAMIC-M [54–56] and Oscura [57], respectively. Existing detector constraints from Migdal effect searches at SENSEI [47,58], XENON10/1T ([60], as shown as in Ref. [58]), CDEX [61,62], and EDELWEISS [63,64] are shown in gray, while Lyman-alpha constraints [59] are shown in blue.
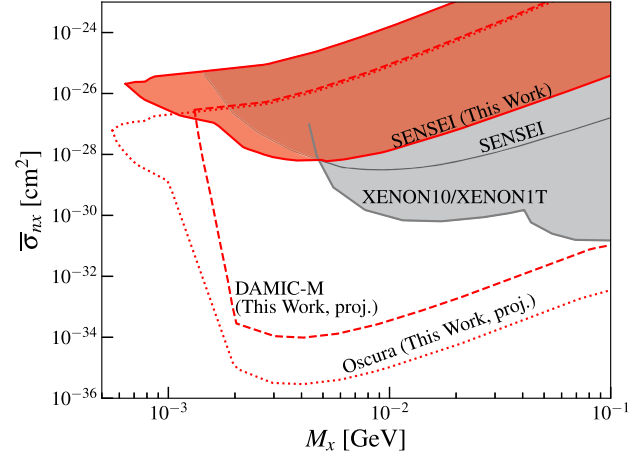

FIG. 3. Limits on the DM-nucleon cross section due to their loop-induced coupling to electrons. Interactions via a light vector mediator with $\alpha_u = -\alpha_d$ and $\alpha_s = 0$. Recast constraints from SENSEI [47] are highlighted in red, and the expected reach of DAMIC-M [54–56] and Oscura [57] are outlined by the red dashed and dotted lines, respectively. Migdal effect constraints from SENSEI [47,58] and XENON10/1T ([60], as shown in Ref. [58]) are shown in gray.

scattering while being only ∼100 m underground [just under 300 m water equivalent (mwe)], presenting a lower overburden than most direct detection experiments. Our limits result from rescaling the reported limits of Ref. [47] by the ratio of the DM-proton and loop-induced DM-electron cross sections found in Eqs. (10) and (12). In the same way, we recast projections for the DAMIC-M experiment [54–56], which has recently released its first results [51], as well as the upcoming Oscura experiment [57].

Figure 2 shows limits and projected sensitivities based on effective loop interactions, for a heavy Z', compared to existing limits from direct detection and cosmology. Our limit constrains DM masses from about 1 to 30 MeV, and is comparable to the strongest existing Migdal effect limit, from SENSEI [47,58], at the lowest masses. It is competitive with the strongest cosmological bounds, which come from Lyman-alpha observations [59]. The projected sensitivities reach cross sections of 10^{-36} cm^2 for masses of a few MeV, orders of magnitude better than existing bounds. For comparison, Ref. [57] shows projections for future Migdal effect searches from the same detectors, but these only extend down to 20 MeV. We also show Migdal effect limits from XENON10 and XENON1T [60], CDEX [61,62], and EDELWEISS [63,64], which provide leading constraints at larger masses.

At the large cross sections we consider, DM may be stopped in the Earth before reaching the detector. While our detection signal relies on scattering with electrons, attenuation will be dominated by scattering with nuclei due to the much larger cross section. We account for attenuation in the

Earth using the ceilings computed for SENSEI in Ref. [13]. These ceiling calculations are also dominated by nuclear scattering, but were computed in a dark photon model. We rescale them by a factor of 4 to account for the scattering with neutrons (assuming typical spin-independent scattering). For DAMIC-M and Oscura, we use the same ceiling, lowered by factors of 17 and 20, respectively, to simulate the overburdens at Laboratoire Souterrain de Modane (4800 mwe) [65] and SNOLAB (6000 mwe) [66].

Figure 3 shows our limits and projected sensitivities for DM models with a light Z', compared to existing limits from direct detection. Cosmological bounds exist on scattering via light mediators, e.g., [67,68] but only at higher cross section. As mentioned above, in the case of a massless mediator, the total cross section diverges, and limits are typically reported in terms of a reference cross section $\bar{\sigma}$. We follow the parametrization of Ref. [13] (see the Supplemental Material for details). In the light Z' case, scattering is typically softer, reducing attenuation in the Earth, so we can constrain a much wider range of parameter space. While Migdal effect bounds from SENSEI and XENON10/XENON1T are stronger than our bounds at large DM masses, our limits dominate for masses up to 5 MeV and extend down well below 1 MeV. Our projections show that DAMIC-M and Oscura can again probe cross sections in the range 10^{-34}–10^{-36} cm^2, competitive with the Migdal effect projections from Ref. [57] and surpassing them for masses below ∼10 MeV (if one were to extrapolate those projections to lower mass). We again show direct detection constraints from SENSEI, XENON10, and XENON1T for comparison. It deserves mention that models of new light Z' mediators coupled to
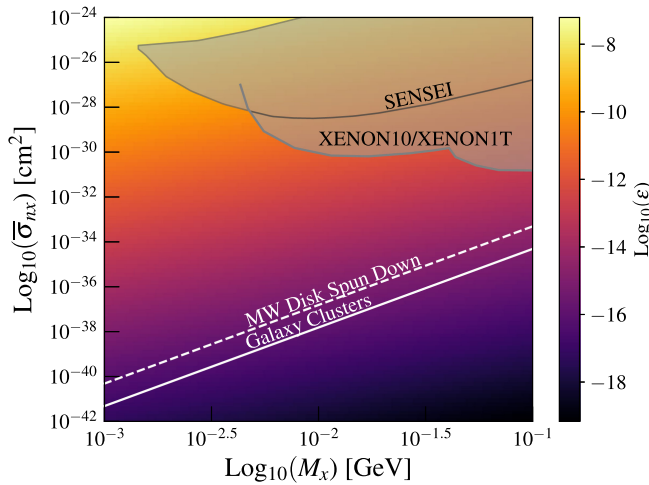
FIG. 4. Effective electric charge resulting from hadronic loop interactions assuming $\alpha_u = -\alpha_d$ and $\alpha_s = 0$. The white lines are astrophysical constraints on millicharged DM: above the solid line, cluster magnetic fields would noticeably alter the density profile of galaxy clusters [72], while above the dashed line, millicharged DM would extract too much angular momentum from the Milky Way disk [71]. The same Migdal effect constraints from Fig. 3 are shown in gray [47,58,60].

baryon currents will also induce SM anomalies that can be constrained through their contribution to rare meson decays [69,70].

Finally, we note that an effectively massless Z' produces an effective fractional electric charge (or "millicharge") for the DM. We can compute the effective charge induced by hadronic loops, and recast limits on millicharged DM as limits on DM-proton interactions via an effectively massless vector. We report our results in terms of ϵ, the DM charge in units of the electron charge, i.e., $q_{\rm DM} = \epsilon e$.

Figure 4 shows, as a color scale, the DM charge corresponding to a given m_χ and $\sigma_{n\chi}$. In gray we superimpose the same Migdal effect limits shown in Fig. 3. Additionally, we show the strongest astrophysical bounds on millicharged DM that can be recast for DM-proton interactions. First, Ref. [71] argued that fractionally charged DM interacting with Galactic magnetic fields in the Milky Way would extract angular momentum from the Milky Way disk, spinning down the disk over the course of gigayears. Although they report an order-of-magnitude uncertainty on their limit, Fig. 4 covers more than 10 orders of magnitude in ϵ. Taking this uncertainty into account, these bounds still far supersede those set by the tree-level interactions. Second, Ref. [72] considered millicharged DM moving in galaxy clusters under the influence of cluster magnetic fields, and argued that if the DM charge were too large, magnetic fields would substantially alter the DM density profile. This results in another strong bound on DM charge, also shown in Fig. 4.

The large DM-proton cross section increases scattering compared to traditional millicharged DM. Thus, not all astrophysical millicharge constraints can apply to the DM considered in this work. For example, constraints from supernova cooling [73] and galactic evacuation due to supernova shocks [74] are severely weakened by enhanced DM-proton scattering. However, we note that enhanced proton scattering could strengthen the astrophysical bounds shown in Fig. 4, by, for example, enhancing the amount of angular momentum extracted from the Milky Way disk.

The couplings of a new vector mediator are subject to a variety of constraints, ranging from meson decay to stellar cooling. References [14,75] compile such constraints for different mass ranges. For a DM mass of 10 MeV, the mediator masses and couplings required to produce our projections in Fig. 3 are easily allowed by the constraints in Ref. [14]: the kinetic mixing parameter is constrained to be below 10^{-9} at 1 MeV, and as large as 10^{-5} for the lowest masses, compared to much smaller values shown in Fig. 4. The couplings needed for the projections in Fig. 2 are comparable to the limits in Ref. [75] (e.g., 10^{-3} at 100 MeV).

Conclusions.—We have presented a 1-loop calculation of the low-energy DM-electron cross section resulting from a tree-level DM-proton interaction. This interaction generically emerges in a wide range of DM models that interact with quarks through a vector mediator. We have used this to derive novel constraints on the DM-proton cross section using existing constraints from SENSEI data. We have shown that currently running and upcoming electron-recoil detectors, DAMIC-M and Oscura, should be sensitive to DM-proton cross sections currently beyond the reach of nuclear recoil detectors. Finally, we have demonstrated that DM that interacts with quarks through a light mediator at tree level has an effective electric charge that can be used to recast astrophysical and cosmological constraints on the DM-electron cross section. Finally, we note that the interactions we have studied could also become evident in electroweak precision tests [76–78], which for a dark photon model have limited $\gamma - Z'$ mixing parameters to $\lesssim \mathcal{O}(10^{-2})$; we leave this to future investigation.

Standard model loop interactions can be an effective tool in exploring DM behavior, and are an inevitable but often-ignored part of any DM theory. While we focused on quark scattering interactions through a vector mediator in this work, we note that other similar loop interactions may be effective at bridging different DM-SM interactions in annihilation processes and with mediators not explored here.

––––––––––

* m.diamond@queensu.ca
† cvc1@queensu.ca
‡ aaron.vincent@queensu.ca
§ joseph.bramante@queensu.ca

[1] G. Bertone, D. Hooper, and J. Silk, Phys. Rep. **405**, 279 (2005).

[2] N. Aghanim *et al.* (Planck Collaboration), Astron. Astrophys. **641**, A6 (2020); **652**, C4(E) (2021).

[3] J. Cooley *et al.*, arXiv:2209.07426.

[4] B. Holdom, Phys. Lett. **166B**, 196 (1986).

[5] A. A. Prinz *et al.*, Phys. Rev. Lett. **81**, 1175 (1998).

[6] S. Davidson, S. Hannestad, and G. Raffelt, J. High Energy Phys. 05 (2000) 003.

[7] M. Pospelov, Phys. Rev. D **80**, 095002 (2009).

[8] S. D. McDermott, H.-B. Yu, and K. M. Zurek, Phys. Rev. D **83**, 063509 (2011).

[9] J. P. Lees *et al.* (*BABAR* Collaboration), Phys. Rev. Lett. **113**, 201801 (2014).

[10] E. Izaguirre and I. Yavin, Phys. Rev. D **92**, 035014 (2015).

[11] M. S. Mahdawi and G. R. Farrar, J. Cosmol. Astropart. Phys. 10 (2018) 007.

[12] J. B. Muñoz and A. Loeb, Nature (London) **557**, 684 (2018).

[13] T. Emken, R. Essig, C. Kouvaris, and M. Sholapurkar, J. Cosmol. Astropart. Phys. 09 (2019) 070.

[14] A. Caputo, A. J. Millar, C. A. J. O'Hare, and E. Vitagliano, Phys. Rev. D **104**, 095029 (2021).

[15] J. Chiles *et al.*, Phys. Rev. Lett. **128**, 231802 (2022).

[16] Y. Kahn and T. Lin, Rep. Prog. Phys. **85**, 066901 (2022).

[17] M. Gorghetto, E. Hardy, J. March-Russell, N. Song, and S. M. West, J. Cosmol. Astropart. Phys. 08 (2022) 018.

[18] A. Romanenko *et al.*, Phys. Rev. Lett. **130**, 261801 (2023).

[19] Z. Bern, P. Gondolo, and M. Perelstein, Phys. Lett. B **411**, 86 (1997).

[20] L. Bergstrom and P. Ullio, Nucl. Phys. **B504**, 27 (1997).

[21] P. Ullio and L. Bergstrom, Phys. Rev. D **57**, 1962 (1998).

[22] F. Boudjema, A. Semenov, and D. Temes, Phys. Rev. D **72**, 055024 (2005).

[23] P. J. Fox and E. Poppitz, Phys. Rev. D **79**, 083528 (2009).

[24] J. Kopp, V. Niro, T. Schwetz, and J. Zupan, Phys. Rev. D **80**, 083502 (2009).

[25] T. Bringmann and C. Weniger, Phys. Dark Universe **1**, 194 (2012).

[26] N. F. Bell, Y. Cai, R. K. Leane, and A. D. Medina, Phys. Rev. D **90**, 035027 (2014).

[27] J. Bramante, N. Desai, P. Fox, A. Martin, B. Ostdiek, and T. Plehn, Phys. Rev. D **93**, 063525 (2016).

[28] E. Charles *et al.* (Fermi-LAT Collaboration), Phys. Rep. **636**, 1 (2016).

[29] J. Kumar and C. Light, J. Cosmol. Astropart. Phys. 07 (2017) 030.

[30] E. Braaten, E. Johnson, and H. Zhang, J. High Energy Phys. 05 (2018) 062.

[31] T. Bringmann, J. Edsjö, P. Gondolo, P. Ullio, and L. Bergström, J. Cosmol. Astropart. Phys. 07 (2018) 033.

[32] H. Abdallah *et al.* (HESS Collaboration), Phys. Rev. Lett. **120**, 201101 (2018).

[33] P. Fileviez Pérez and C. Murgui, Phys. Rev. D **100**, 123007 (2019).

[34] A. Albert *et al.* (HAWC Collaboration), Phys. Rev. D **101**, 103001 (2020).

[35] C. Arina, B. Fuks, and L. Mantani, Eur. Phys. J. C **80**, 409 (2020).

[36] L. Rinchiuso, O. Macias, E. Moulin, N. L. Rodd, and T. R. Slatyer, Phys. Rev. D **103**, 023011 (2021).

[37] C. Arina, J. Heisig, F. Maltoni, D. Massaro, and O. Mattelaer, Eur. Phys. J. C **83**, 241 (2023).

[38] J. W. Foster, Y. Park, B. R. Safdi, Y. Soreq, and W. L. Xu, Phys. Rev. D **107**, 103047 (2023).

[39] J. Kopp, L. Michaels, and J. Smirnov, J. Cosmol. Astropart. Phys. 04 (2014) 022.

[40] K. A. Mohan, D. Sengupta, T. M. P. Tait, B. Yan, and C. P. Yuan, J. High Energy Phys. 05 (2019) 115; 05 (2023) 232(E).

[41] See Supplemental Material at http://link.aps.org/supplemental/10.1103/PhysRevLett.132.051001 for detailed derivations of the tree level and loop level cross sections used in this work, and show the constraints accessible for dark matter which interacts with protons but not pions.

[42] F. Jegerlehner, *The Anomalous Magnetic Moment of the Muon* (Springer, Cham, 2017), Vol. 274, 10.1007/978-3-319-63577-4.

[43] T. Becher and H. Leutwyler, Eur. Phys. J. C **9**, 643 (1999).

[44] R. Essig, T. Volansky, and T.-T. Yu, Phys. Rev. D **96**, 043017 (2017).

[45] A. Aguilar-Arevalo *et al.* (DAMIC Collaboration), Phys. Rev. Lett. **123**, 181802 (2019).

[46] E. Aprile *et al.* (XENON Collaboration), Phys. Rev. Lett. **123**, 251801 (2019).

[47] L. Barak *et al.* (SENSEI Collaboration), Phys. Rev. Lett. **125**, 171802 (2020).

[48] C. Cheng *et al.* (PandaX-II Collaboration), Phys. Rev. Lett. **126**, 211803 (2021).

[49] E. Aprile *et al.* (XENON Collaboration), Phys. Rev. D **106**, 022001 (2022).

[50] P. Agnes *et al.* (DarkSide Collaboration), Phys. Rev. Lett. **130**, 101002 (2023).

[51] I. Arnquist *et al.* (DAMIC-M Collaboration), Phys. Rev. Lett. **130**, 171003 (2023).

[52] P. Agrawal, Z. Chacko, C. Kilic, and R. K. Mishra, arXiv:1003.1912.

[53] G. Ecker, J. Gasser, A. Pich, and E. de Rafael, Nucl. Phys. **B321**, 311 (1989).

[54] M. Battaglieri *et al.*, in U.S. Cosmic Visions: New Ideas in Dark Matter (2017), arXiv:1707.04591.

[55] M. Settimo (DAMIC Collaboration), in *Proceedings of the 53rd Rencontres de Moriond on Cosmology* (2018), pp. 315–318; arXiv:1805.10001.

[56] M. Settimo (DAMIC and DAMIC-M Collaborations), in *Proceedings of the 16th Rencontres du Vietnam: Theory meeting experiment: Particle Astrophysics and Cosmology* (2020); arXiv:2003.09497.

[57] A. Aguilar-Arevalo *et al.*, arXiv:2202.10518.

[58] K. V. Berghaus, A. Esposito, R. Essig, and M. Sholapurkar, J. High Energy Phys. 01 (2023) 023.

[59] K. K. Rogers, C. Dvorkin, and H. V. Peiris, Phys. Rev. Lett. **128**, 171301 (2022).

[60] R. Essig, J. Pradler, M. Sholapurkar, and T.-T. Yu, Phys. Rev. Lett. **124**, 021801 (2020).

[61] Z. Z. Liu *et al.* (CDEX Collaboration), Phys. Rev. Lett. **123**, 161301 (2019).

[62] Z. Z. Liu *et al.* (CDEX Collaboration), Phys. Rev. D **105**, 052005 (2022).

[63] E. Armengaud *et al.* (EDELWEISS Collaboration), Phys. Rev. D **99**, 082003 (2019).

[64] E. Armengaud *et al.* (EDELWEISS Collaboration), Phys. Rev. D **106**, 062004 (2022).

[65] F. Piquemal, Eur. Phys. J. Plus **127**, 110 (2012).

[66] F. Duncan, A. J. Noble, and D. Sinclair, Annu. Rev. Nucl. Part. Sci. **60**, 163 (2010).

[67] E. D. Kovetz, V. Poulin, V. Gluscevic, K. K. Boddy, R. Barkana, and M. Kamionkowski, Phys. Rev. D **98**, 103529 (2018).

[68] T. R. Slatyer and C.-L. Wu, Phys. Rev. D **98**, 023013 (2018).

[69] J. A. Dror, R. Lasenby, and M. Pospelov, Phys. Rev. D **96**, 075036 (2017).

[70] J. A. Dror, R. Lasenby, and M. Pospelov, Phys. Rev. D **99**, 055016 (2019).

[71] A. Stebbins and G. Krnjaic, J. Cosmol. Astropart. Phys. 12 (2019) 003.

[72] K. Kadota, T. Sekiguchi, and H. Tashiro, arXiv:1602.04009.

[73] J. H. Chang, R. Essig, and S. D. McDermott, J. High Energy Phys. 09 (2018) 051.

[74] L. Chuzhoy and E. W. Kolb, J. Cosmol. Astropart. Phys. 07 (2009) 014.

[75] S. Knapen, T. Lin, and K. M. Zurek, Phys. Rev. D **96**, 115021 (2017).

[76] A. Hook, E. Izaguirre, and J. G. Wacker, Adv. High Energy Phys. **2011**, 859762 (2011).

[77] D. Curtin, R. Essig, S. Gori, and J. Shelton, J. High Energy Phys. 02 (2015) 157.

[78] B. M. Loizos, X. G. Wang, A. W. Thomas, M. J. White, and A. G. Williams, arXiv:2306.13408.